

Human Video Translation via Query Warping

Haiming Zhu
Tsinghua University
Shenzhen, China

zhm21@mails.tsinghua.edu.cn

Yangyang Xu
The University of Hong Kong
Hong Kong

Shengfeng He
Singapore Management University
Singapore

Abstract

In this paper, we present QueryWarp, a novel framework for temporally coherent human motion video translation. Existing diffusion-based video editing approaches that rely solely on key and value tokens to ensure temporal consistency, which scarifies the preservation of local and structural regions. In contrast, we aim to consider complementary query priors by constructing the temporal correlations among query tokens from different frames. Initially, we extract appearance flows from source poses to capture continuous human foreground motion. Subsequently, during the denoising process of the diffusion model, we employ appearance flows to warp the previous frame’s query token, aligning it with the current frame’s query. This query warping imposes explicit constraints on the outputs of self-attention layers, effectively guaranteeing temporally coherent translation. We perform experiments on various human motion video translation tasks, and the results demonstrate that our QueryWarp framework surpasses state-of-the-art methods both qualitatively and quantitatively.

1. Introduction

Given a human action video, transferring its motion to another human to synthesize a new video has received much attention and made great progress in the community of computer vision and graphics. Existing works [2, 4, 5, 20, 23, 29, 36] utilize Generative Adversarial Networks (GANs)[10], taking the reference action video and target frame as conditional inputs. However, the translated videos resemble the target frames and cannot be edited using text[24]. Recently, Text-to-Image (T2I) diffusion models [26, 28, 32] have gained significant progress in static image synthesis. Given a text prompt, a vivid image can be generated in various styles. Moreover, ControlNet [40] em-

powers T2I’s control ability with various conditions beyond the text prompt.

Based on the generative and controllable ability of the T2I diffusion model, one can transfer human motions to another person using pose guidance. However, directly transferring each frame will lead to temporal inconsistency across frames. To preserve the temporal consistency of translated frames, recent works [37, 39] have designed a cross-frame attention mechanism on the latent tokens to maintain temporal coherence. Particularly, they share the *key* and *value* tokens across frames in the self-attention layer of the Stable Diffusion model [30]. While global coherence can be preserved using the cross-frame attention mechanism, local consistency remains a challenge. For example, ControlVideo2 [42] presents inconsistent jeans in the 2nd sample of Fig. ???. This is because each frame’s *query* token is adopted from the current frame. As analyzed in[3], the *query* token controls the layout and structure of the object. Motivated by this observation, in order to obtain a temporally coherent translated motion video, we seek to leverage and optimize the consistency between queries.

In this paper, we propose *QueryWarp*, a flow-guided attention mechanism that warps the *query* token in self-attention layer using dense flows, for the temporal coherent human motion video translation. Given a source human motion video, we first extract the conditions (*i.e.*, poses, HED boundaries, and *et al.*) from the video, and use ControlNet [40] to transfer human motions. To guarantee the temporal consistency of translated video, we predict the dense flows between two adjacent frames or poses and use them as a constraint to ensure temporally coherent translation. Unlike Rerender A Video [39] that applies optical flow on different stages of diffusion sampling stages, we warp the query tokens of different frames in diffusion’s denoising process. Particularly, in each frame, we warp the *query* token from the last frame and fuse with the current *query*

according to an occlusion mask. In this way, the human body regions of two adjacent frames have smooth content. Together with the cross-frame mechanism that shares *key* and *value* across different frames, our *QueryWarp* obtains the temporal coherent outputs of the attention layer, which guarantees the temporal consistency of translated videos. Moreover, our method does not require training or fine-tuning the diffusion model on a specific video, preserving the powerful generative ability of original T2I diffusion models. Meanwhile, it also can be applied to the noisy latent codes or inverted latent codes. We conduct experiments on human motion translation tasks with various styles provided by text prompts, and the extensive experiments demonstrate the superiority over state-of-the-art methods in terms of quantitative and qualitative evaluations.

In summary, our contributions are three-fold:

- We propose *QueryWarp*, a novel framework for human motion video translation. It enforces the temporal coherence of translated videos by introducing dense flows into self-attention layer of the diffusion model.
- We analyze that the inconsistency of different frames is aroused by the inconsistency *query* tokens across different frames, and introduce the flows to warp the query tokens for guaranteeing the temporal coherent translation.
- Extensive experiments demonstrate that our *QueryWarp* achieves state-of-the-art performance on human motion translations.

2. Related Work

Diffusion Models. Diffusion models [1, 6, 11, 18, 30] receive significant attention due to its generative ability. Beginning with random noise, these models progressively denoise it to generate a sample. Recently, diffusion-based T2I models [26, 28, 32] achieve a new stage in image synthesis. Particularly, Latent Diffusion model [30] performs diffusion process in the variational auto-encoder’s [19] latent space and synthesizes high-quality image with a text prompt. Hence many works [3, 12, 37, 41] utilize its generative ability on real image or video editing.

Diffusion-based Video Generation and Editing. While diffusion models achieve significant generative ability, several works apply this ability to video generation or editing. Video Diffusion Models [15] propose a space-time U-Net for performing diffusion on pixels. Imagen Video [13] successfully generates high-quality videos with cascaded diffusion models and v-prediction parameterization. Make-A-Video [34] combines the appearance generation of T2I models with movement information from video data. Recent works [7, 8] have commenced exploring the re-training of the T2I model using video data, aiming to enable text-to-video functionality. As for video editing, preserving the temporal consistency of edited videos is es-

sential but challenging. For improving the temporal consistency, Tune-A-Video [37] inflates the 2D U-Net to 3D for modeling temporal information, meanwhile proposes a temporal attention mechanism. VideoP2P [21] builds upon the inflated model and utilizes Prompt-to-Prompt [12] editing on the tuned model. Fatezero [27] implements zero-shot text-driven video editing through the blending attention mechanism. By introducing additional spatial guidance using ControlNet [40], Rerender A Video [39] proposes a text-guided video-to-video translation framework aimed at adapting image models to videos. ControlVideo2 [42] introduces key-frame and attention to video-to-video translation. Follow your pose [24] introduces the T2I diffusion model in pose-guided text-to-image generation, and further extends into video generation by adding the learnable temporal attention into the T2I model. However, most of those works build the temporal attention mechanism by the shared *key* and *value* tokens but ignore the essential temporal consistency in *query* tokens. Recently, TokenFlow [9] propagates features from the keyframe to other frames based on the source video features’ correspondence. However, if the source and target prompts have a large domain gap, the source correspondences cannot be used for guidance in the target videos. We extract appearance flows from the shared pose sequence, which is agnostic to large prompt gaps.

Human Motion Translation. Generating a human video from the driving signal has been widely studied. Early works transfer human video pose to a target person using GANs. Vid2vid [36] introduces the optical flow and temporal consistency constraints that translate source video to target one. Chan *et al.* [4] use two consecutive frames for temporally coherent video translation. Combining the source image with the source pose as inputs, some methods [2, 5, 20, 23, 29] predict motion flows based on poses or frames and perform pose transfer using a warp module. FOMM [33] animates a given image by proposing a first-order motion representation. Nevertheless, these methods can only translate the videos with the given image style but fail to translate various video styles controlled by text prompts.

3. Approach

3.1. Preliminaries

Latent Diffusion Models(LDMs) is a text-to-image model that conducts a diffusion process in the latent space of an autoencoder. It has an autoencoder and a Denoising Diffusion Probabilistic Model (DDPM) [14]. Given an image x , it first is encoded to a latent code z through an autoencoder \mathcal{E} , *i.e.*, $z = \mathcal{E}(x)$. In the forward diffusion process, the DDPM adds Gaussian noise to the latent code z iteratively:

$$q(z_t|z_{t-1}) = \mathcal{N}(z_t; \sqrt{1 - \beta_t}z_{t-1}, \beta_t I),$$

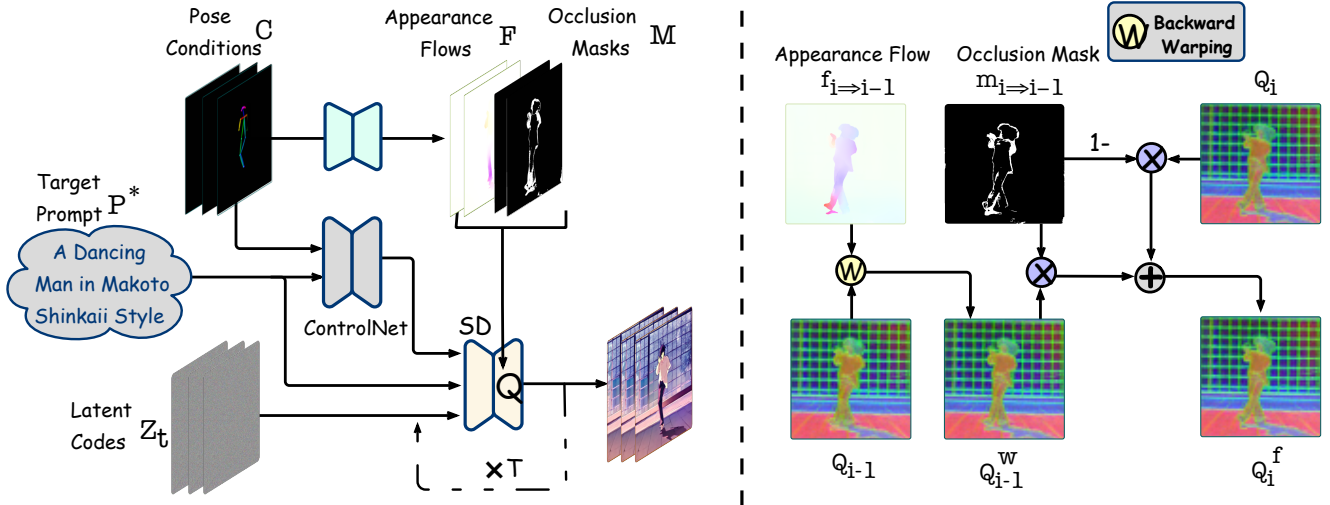


Figure 1. Left: Pipeline of our *QueryWarp*. Given a pose sequence \mathcal{C} , we first predict the appearance flow \mathcal{F} and occlusion mask \mathcal{M} using [20]. Then we feed the pose sequence condition \mathcal{C} and target prompt \mathcal{P}^* to ControlNet which controls the outputs of Stable Diffusion. In each denoising process, we warp the *query* tokens in U-Net decoder’s self-attention layers using appearance flow. Right: Details of our *flow-guided attention*, in each timestep i , we warp its last timestep’s *query* token Q_{i-1} using flow $f_{i \Rightarrow i-1}$, and then fuse warped results Q_{i-1}^w with current *query* token Q_i according to occlusion mask $m_{i \Rightarrow i-1}$ to get the final coherent *query* token Q_i^f .

where $q(z_t|z_{t-1})$ is the conditional density of z_t given z_{t-1} , $\{\beta_t\}_{t=0}^T$ are the scale of noises, and T is the total timestep of the diffusion process.

The backward denoising process is represented as:

$$p_\theta(z_{t-1}|z_t) = \mathcal{N}(z_{t-1}; \mu_\theta(z_t, t), \Sigma_\theta(z_t, t)),$$

where the μ_θ and Σ_θ are implemented with denoised model ϵ_θ , it is trained using following objective:

$$\mathbb{E}_{z, \epsilon \sim \mathcal{N}(0,1), t} [\|\epsilon - \epsilon_\theta(z_t, t, c_{\mathcal{P}})\|_2^2], \quad (1)$$

where $c_{\mathcal{P}}$ is the text prompt.

DDIM Sampling and Inversion During inference, deterministic DDIM sampling [35] is employed to progressively convert a random Gaussian noise z_T to a clean latent code z_0 with following equation:

$$z_{t-1} = \sqrt{\alpha_{t-1}} \frac{z_t - \sqrt{1 - \alpha_t} \epsilon_\theta}{\sqrt{\alpha_t}} + \sqrt{1 - \alpha_{t-1}} \epsilon_\theta,$$

where t is denoising step $t : T \rightarrow 1$ and α_t is a parameter for noise scheduling [14, 35].

To reconstruct real images and perform editing [12, 25], DDIM inversion [6] is employed to encode a real image latent code z_0 to related inversion noise by reversing the above process in reversed steps $t : 1 \rightarrow T$.

ControlNet is a conditional text-to-image generative model, capable of handling various conditions $c_{\mathcal{F}}$, e.g., depth maps, poses, edges. By constructing the noise prediction network $\epsilon_\theta(z_t, t, c_{\mathcal{P}}, c_{\mathcal{F}})$, ControlNet [40] adds a trainable copy encoding model for the conditional input $c_{\mathcal{F}}$. It then utilizes zero-convolutions connected with the prompt input $c_{\mathcal{P}}$ for task-specific conditional image generation.

3.2. Procedure

Give a source human actions video $\mathcal{V} = \{v_i \mid i \in [1, N]\}$ with N frames, our goal is to translate it to a target temporal coherent video \mathcal{V}^* under the pose condition $\mathcal{C} = \{c_i \mid i \in [1, N]\}$ that aligns with the target prompt \mathcal{P}^* , meanwhile retains the sequential human actions from the source video. Different from existing works [4, 22] take the additional reference image as input, our translated video appearance is controlled by the given target prompt \mathcal{P}^* and the pose guidance \mathcal{C} . The pipeline of our *QueryWarp* is shown in the left part of Fig. 1, we build the framework based on Stable Diffusion [30] and ControlNet [40]. We first follow Tune-A-Video [37] that inflates the 2D U-Net [31] of the T2I model to pseudo-3D U-Net, and we further reprogram the self-attention layer with the appearance flows into a flow-guided attention for preserving the temporal consistency of translated videos.

3.2.1 Self-Attention Mechanism

Before introducing our method, we would like to introduce the attention mechanism of the original T2I model at first. In specific, given the latent representation z_i of frame i , the original self-attention mechanism first projects it to *query*, *key*, and *value* tokens (Q_i , K_i , and V_i) respectively. Then the self-attention mechanism is presented as:

$$Q_i = W^Q z_i, K_i = W^K z_i, V_i = W^V z_i,$$

$$\text{Attn}(Q_i, K_i, V_i) = \text{SoftMax}\left(\frac{Q_i K_i^T}{\sqrt{d}}\right) \cdot V_i,$$

where W^Q , W^K , and W^V project z_i into *query*, key, value respectively, and d is the output dimension of key and *query* tokens.

The self-attention mechanism handles each frame individually, which cannot guarantee the temporal consistency of frames. To eliminate the content inconsistency, existing T2I-based video editing works [37, 42] select a keyframe and propagate its content to other frames. Particularly, they replace the key and value tokens of different frames using an anchor frame’s token, that is, they extend the self-attention to cross-frame attention using the shared anchor key and value tokens. Specifically, on frame i , the cross-frame attention can be presented as:

$$\text{CFAttn}_i = \text{SoftMax}\left(\frac{Q_i K_{anc}^T}{\sqrt{d}}\right) \cdot V_{anc}, \quad (2)$$

where K_{anc} and V_{anc} denotes the selected anchor key and value tokens. However, the temporal inconsistency cannot be eliminated due to the *query* token Q_i is adopted from the current frame, but there are no explicit constrains applied to different frames’ *query* tokens. In this paper, we reprogram the cross-frame attention mechanism into a flow-guided attention mechanism that builds the temporal correlations on the *query* tokens to eliminate the temporal inconsistency.

3.2.2 Flow-guided Attention

As shown in the left part of Fig. 1, we first extract the flow motions from the source video. A direct way is to extract optical flows from the source video \mathcal{V} . However, in the text-guided motion translation, the target text prompt may be very different from the source video. Take Fig. ?? as an example, the prompt of source video is “*a man is dancing*”, but the target prompt is “*a panda is dancing with a moon background*”. In this case, the optical flows extracted from the video frames cannot describe the temporal correspondence of “*panda*” is different from the “*man*” due to the structure differences. In this case, optical flows cannot be used for warping queries.

We notice the pose sequence can be shared regardless of the domain gap, and the appearance flow also can be predicted by the poses sequence. Here we predict the appearance flows on the pose sequence $\mathcal{C} = \{C_i \mid i \in [1, N]\}$ using [20] and obtain the flow sequences $\mathcal{F} = \{f_{i \Rightarrow i-1} \mid i \in [2, N]\}$. Meanwhile, the pose sequence $\mathcal{C} = \{C_i \mid i \in [1, N]\}$ maps $\mathcal{M} = \{m_i \mid i \in [1, N]\}$ also can be predicted by [20]. Based on the appearance flows and occlusion maps, we build the temporal correlations among different frames’ *query* tokens.

As shown in the right part of Fig. 1, in the frame i , we first warp the last frame’s *query* Q_{i-1} using the resized flow $f_{i \Rightarrow i-1}$ ¹, and then fuse the warped result with the original

¹Here we use $f_{i \Rightarrow i-1}$ to denote original and resized flows for simplify.

query token Q_i according to the occlusion map $m_{i \Rightarrow i-1}$:

$$Q'_{i-1} = \mathbb{W}(Q_{i-1}, f_{i \Rightarrow i-1}),$$

$$Q_i^f = m_{i \Rightarrow i-1} \cdot Q'_{i-1} + (1 - m_{i \Rightarrow i-1}) \cdot Q_i,$$

where $\mathbb{W}(\cdot, \cdot)$ is the backward warpping operation, Q'_{i-1} is the warped results of *query* token Q_{i-1} , and Q_i^f is the fused *query* token. Now we define the flow-guided attention by replacing the Q_i in Eq. 2 with Q_i^f :

$$\text{FGAttn}_i = \text{SoftMax}\left(\frac{Q_i^f K_{anc}^T}{\sqrt{d}}\right) \cdot V_{anc}.$$

We apply flow-guided attention on SD’s U-Net decoder [3, 40], in our flow-guided attention, the flow controls the *query* tokens across different frames, and together with sharing value and key tokens across different frames, the temporal coherence can be preserved effectively.

For that translation that has less domain gap, we also use the HED boundaries as conditions. Under this condition, we use the optical flows extracted from the video frames using GMFlow [38], and we follow [16, 39] that calculates the occlusion map based on warp error.

4. Experiments

4.1. Implementation Details

Implementation details. We collect 40 human motion videos from the Internet, which consist of dancing and sports-related videos. Then we manually add the caption to form text-video pairs. The Stable Diffusion 1.5 [30] and ControlNet 1.0 [40] are adopted in our framework. Following previous works [37, 42], we sample 8 frames with 512×512 resolution from each video. During sampling, a DDIM sampler with 50 steps and 12 classifier-free guidance is used for inference.

Metrics. In our evaluation, three metrics are utilized to assess text alignment, temporal consistency, and pose accuracy, which includes: i) Editing Accuracy (**Editing-Acc**): This metric represents the frame-wise editing accuracy. We calculate the similarity between translated frames and source and target prompts respectively. If the target similarity is higher than source similarity indicates a successful editing. ii) Temporal Consistency (**Tem-Con**): This metric calculates the cosine similarity between all pairs of consecutive frames. iii) Pose Distance (**Pose-Dist**): We use this metric to evaluate whether the motion is corrected transferred. It calculates the L2 distance between pose key points of the source and translated videos.

Competitors. We compare our QueryWarp with several zero-shot and one-shot related works. The zero-shot methods include Rerender A Video [39], ControlVideo1 [41], TokenFlow [9], Text2Video-Zero [17],



Figure 2. Qualitative comparisons with zero-shot video methods. Our QueryWarp captures the pose condition and prompt style correctly.

Follow-Your-Pose [24], and FateZero [27], above methods don’t need to finetune the diffusion model on the source video. One-shot methods include Tune a Video [37], ControlVideo2 [42], VideoP2P [21], which finetunes the diffusion model on each source video. In the comparison, we either zero or one-shot setting on our QueryWarp depending on the compared methods for a fair comparison. In addition, our method can both take DDIM inverted codes or random noise as initial latent codes.

4.2. Qualitative Comparisons

We first present the comparison with zero-shot methods in Fig. 2, we can see that Follow-Your-Pose [24] captures the global style of target prompts, but fails to keep the pose controls. FateZero [27] and TokenFlow [9] fail to capture the prompt styles. In contrast, our QueryWarp accurately captures the motions from the source sequence, meanwhile capturing the target prompts effectively.

The comparison with one-shot competitors is shown in Fig. 3, our QueryWarp demonstrates significant editing capabilities across a large domain through one-shot tuning. In the 2_{nd} sample, both VideoP2P and Tune A Video fail to generate the “moon”. That is because VideoP2P [21] can only perform local editing by introducing an editing mask, and Tune A Video heavily fine-tune SD on a source

video (about 300 steps) to capturing its temporal correlation, but degenerates the generative ability of SD. ControlVideo2 [42] synthesis the “moon” with the “hand” misalignment (see red box in 2_{nd} sample). Our QueryWarp captures temporal correlations of a video without harm SD’s generative ability, which allows to addition of new objects meanwhile preserving the temporal coherence.

As mentioned in Sec. 3.2.2, our method can also use the optical flows to warping instead of appearance flow when source and target prompts have less domain gap. We also experimented using optical flows. In this experiment, we take the HED boundaries as a condition, and the random noise is employed as initial latent codes. The comparison with can be seen in Fig. 4. Tough all methods capture the prompt styles and pose condition to some extent, Text2Video-Zero [17] present artifacts around hairs, ControlVideo1 [41] misses feet or arm (see in red box of Fig. 4), and Rerender A Video [39] presents discontinuous hair and background colors in the last frame. Our QueryWarp achieves high-quality translation on each frame meanwhile preserving temporal consistency across different frames, which indicates our model is robust to different flows and random latent codes.

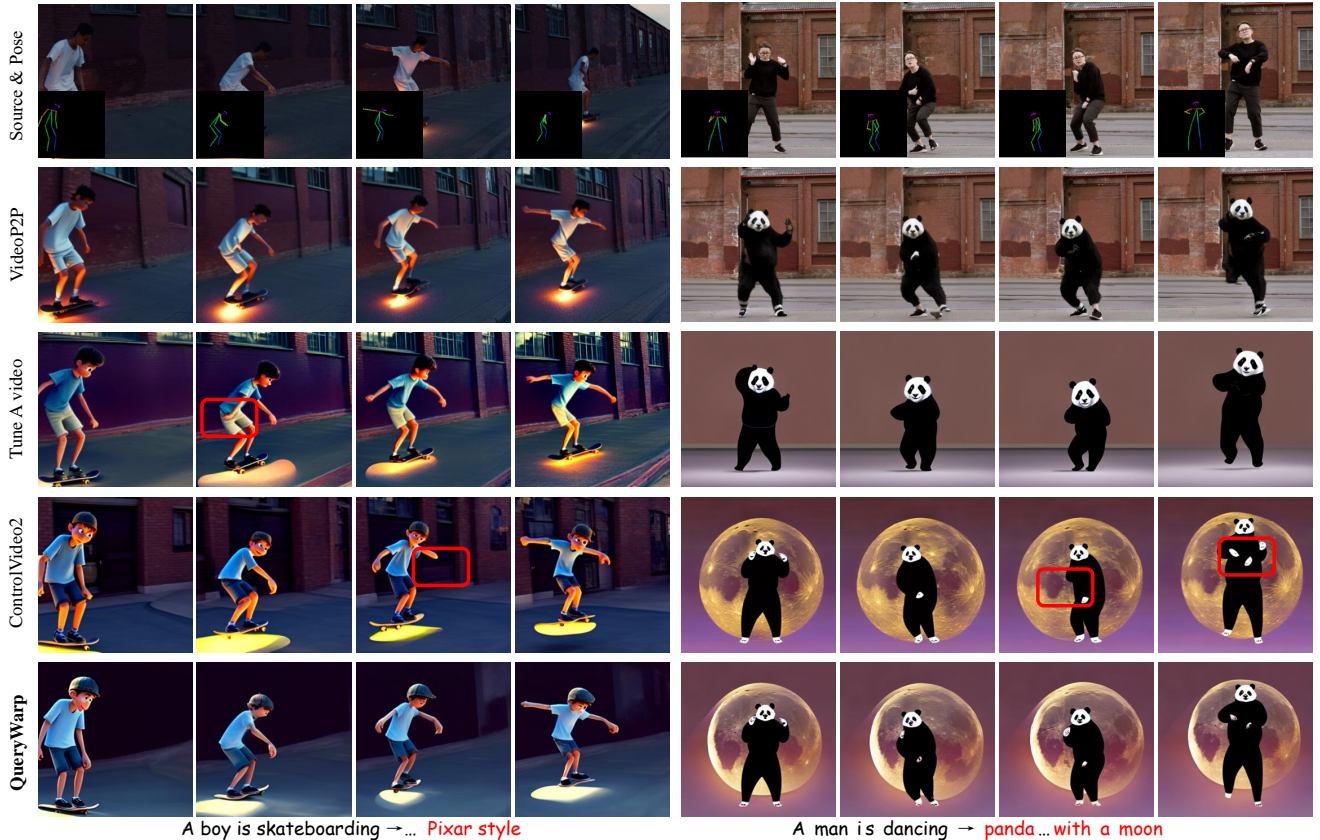


Figure 3. Qualitative comparisons with one-shot video methods. QueryWarp aligns with the pose condition and synthesizes new objects.

Table 1. Quantitative comparisons with zero-shot methods.

Methods	Tem-Con \uparrow	Editing-Acc \uparrow	Pose-Dist \downarrow
TokenFlow [9]	0.9358	0.9417	32.1720
FateZero [27]	0.9390	0.6154	22.0665
Follow your pose [24]	0.9501	0.9640	64.4661
QueryWarp	0.9563	0.9429	28.5438

Table 2. Quantitative comparisons under one-shot setting.

Methods	Tem-Con \uparrow	Editing-Acc \uparrow	Pose-Dist \downarrow
Tune a video [37]	0.9575	0.8432	31.4616
VideoP2P [21]	0.9575	0.6708	29.9871
ControlVideo2 [42]	0.9590	0.9428	31.0421
QueryWarp	0.9658	1	29.4123

4.3. Quantitative Comparisons

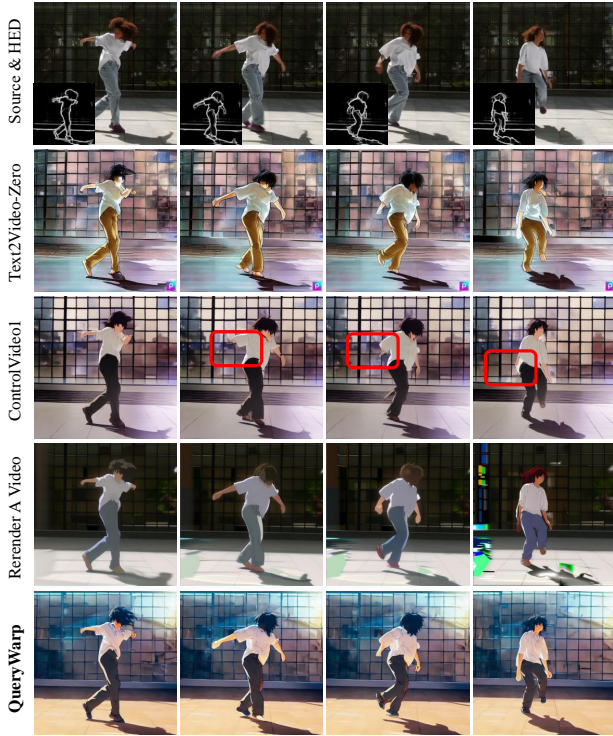
The quantitative comparison with zero-shot methods is shown in Tab. 1, QueryWarp achieves a balance between temporal consistency and accurate editing, showing results comparable to TokenFlow [9]. Particularly, TokenFlow [9] performs significantly worse in terms of pose distance compared to our method. FateZero [27] has the best performance on the Pose-Dist metric due to its worse performance on style-related translation, as demonstrated in Fig. 2, it cannot achieve the successful style translation on *Van Gogh style*. Follow-Your-Pose [24] achieves the highest semantic editing accuracy but has the largest pose distance, which indicates it cannot be controlled by pose effectively. In contrast, our QueryWarp combines ControlNet [40] to achieve better pose control, and the introduction of pose flow allows us to

Table 3. Quantitative comparisons using random noise as initial latent codes with HED boundary conditions.

Methods	Tem-Con \uparrow	Editing-Acc \uparrow	Pose-Dist \downarrow
Rerender A Video [39]	0.9648	0.6879	17.0119
Text2Video-Zero [17]	0.9597	1	16.3427
ControlVideo1 [41]	0.9741	1	15.0137
QueryWarp	0.9697	1	12.0414

perform zero-shot video editing.

Tab. 2 presents the quantitative comparison under one-shot setting, Tune a Video [37] and VideoP2P [21] heavily rely on finetuning on the source video, struggle to balance pose control and editing capabilities, resulting in lower editing accuracy. QueryWarp utilizes flow to construct consis-



A person is dancing → ... *Makoto Shinkai style*

Figure 4. Qualitative comparisons with three competitors using random noise as initial latent codes. In this comparison, we use the optical flow and HED boundaries in our QueryWarp.

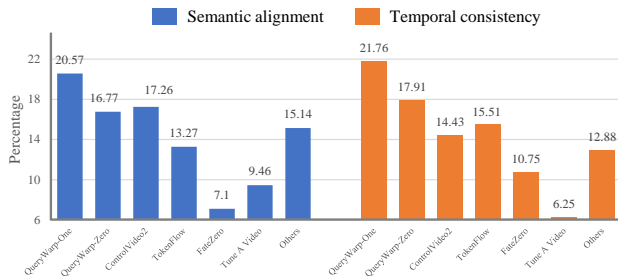
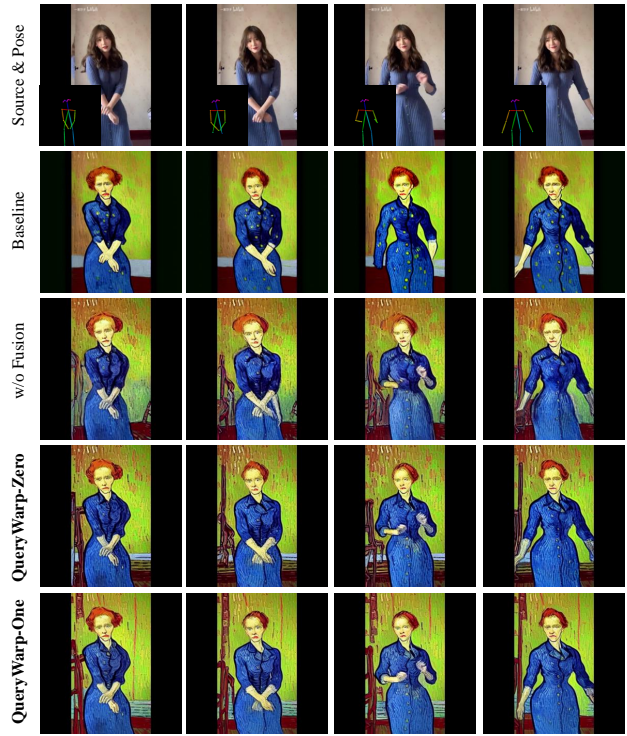


Figure 5. Results of the user studies. We show the percentage of preferred votes over different methods.

tency between *query* tokens across two frames and achieves the best temporal consistency, editing accuracy, and lowest pose distance.

The quantitative comparison by taking random noise as initial latent codes is shown in Tab. 3, Render A Video [39] utilizes optical flow to warp in pixel-level, it still presents color distortion and discontinuous. ControlVideo1 [41], with its full attention mechanism, struggles to maintain temporal consistency of fine-grained structure, resulting in the issue of missing hands and legs in intermediate frames. In contrast, combining HED conditions and optical flow, QueryWarp exhibits robust performance in both consistency and editing accuracy.



A beautiful woman → ..., *Van Gogh style*

Figure 6. Qualitative comparison with different variants. Each of the components contributes to our final model.

4.4. User Study

We also introduce the user study for the objective evaluation. The user studies involved 45 participants being asked two questions. Specifically, we provide participants with source videos, target text prompts, and translated videos obtained from all methods. For each source video, we require participants to assess its translated videos from two perspectives: i) the semantic alignment, participants are asked to choose which translated video is the most semantic alignment with the given target prompt. ii) the temporal consistency, raters need to select the most temporal consistency video from all translated videos. The average preference rates can be seen in Fig. 5. In each sub-figure, we only present the top six methods; the rest are summarized into “others”. We can see that FateZero [27] receives lower semantic alignment votes as it cannot achieve successful translations. TokenFlow [9] introduces feature correspondence into translation, and its temporal consistency can be well preserved, resulting in a higher preference in all competitors on temporal consistency evaluation. Both QueryWarp-One and QueryWarp-Zero outperform the others on two tasks including semantic alignment and temporal consistency, demonstrating our flow-guided attention’s effectiveness.

Table 4. Quantitative comparison of various variants.

Method	Tem-Con \uparrow	Editing-Acc \uparrow	Pose-Dist \downarrow
Baseline	0.9284	0.9053	35.9950
<i>w/o</i> fusion	0.9416	0.9217	30.1251
QueryWarp-Zero	0.9563	0.9429	28.5439
QueryWarp-One	0.9658	1	29.4123

4.5. Ablation Study

To evaluate the effectiveness of different components in our QueryWarp, we conduct ablation studies in this section. We first set a baseline by using cross-frame attention instead of our flow-guided attention. Moreover, we also remove the fusion operation according to the occlusion map after backward wrapping (*w/o* fusion), that is, we use the last frame’s warped *query* as the current frame’s *query*. We experiment above variants under zero-shot setting. In addition, for evaluating the necessity of fine-tuning on a specific video, we also compare our method under zero- and one-shot settings, denoted by QueryWarp-Zero and QueryWarp-One respectively.

The qualitative comparison among different variants can be seen in Fig. 6, cooperating ControlNet [40] and cross-frame attention, the baseline model can roughly perform video editing, but issues such as multiple hands still exist. In contrast, variant *w/o* fusion correctly corrects the limbs but introduces pseudo artifacts from the previous frame (evident from the hair). Thanks to flow-guided attention, QueryWarp-Zero accurately maps the human body pose without introducing any pseudo artifacts. We also find that QueryWarp-Zero and QueryWarp-One present similar visual results in Fig. 6, which indicates that our QueryWarp learns the temporal correlation by the flow-guided attention but not overfitting on a specific video.

We also conducted quantitative experiments on different variants, as shown in Tab. 4. Compared with the baseline, variant *w/o* fusion has a lower Pose-Dist value, which indicates that our flow-guided attention reduces the pose distance significantly. Meanwhile, variant QueryWarp-Zero has a better performance than variant *w/o* fusion on the Tem-Con metric, which indicates the necessity of introducing an occlusion mask. Moreover, we also find that QueryWarp-Zero receives a similar performance with QueryWarp-One, especially on Tem-Con and Pose-Dist metrics, which indicates that our method is agnostic to fine-tuning SD on source video.

5. Conclusion, Limitation, and Future Work

In this paper, we present QueryWarp, a novel framework for temporally coherent human motion video translation. By identifying the inconsistency of *query* tokens in SD’s self-attention layer across different frames as a key challenge,

we introduce appearance flow extracted from the pose sequence to warp the last frame’s *query* token. We then fuse the warped result with the current frame’s *query* token according to the occlusion mask. By addressing *query* token inconsistency and introducing dense flows, our approach outperforms existing methods in both qualitative and quantitative evaluations.

Our warping process depends on the quality of the off-the-shelf appearance flow detector and occlusion masks. While we have made efforts to ensure the accuracy of our approach, the performance of our framework can be influenced by the accuracy and robustness of these external components. In cases where the appearance flow detector fails to accurately capture motion, or where occlusion masks are not precise, it can lead to challenges in achieving optimal temporal coherence. Future work in this area could involve developing more advanced optical flow detection techniques or refining the occlusion mask generation process to improve the robustness of our framework. Additionally, exploring the integration of alternative sources of motion information, such as pose estimations or scene understanding, could further enhance the reliability and versatility of our approach. These considerations will be central to our ongoing efforts to address and mitigate these limitations and extend the applicability of our framework.

References

- [1] Jacob Austin, Daniel D Johnson, Jonathan Ho, Daniel Tarlow, and Rianne van den Berg. Structured denoising diffusion models in discrete state-spaces. In *NeurIPS*, volume 34, pages 17981–17993, 2021. 2
- [2] Guha Balakrishnan, Amy Zhao, Adrian V Dalca, Fredo Durand, and John Guttag. Synthesizing images of humans in unseen poses. In *CVPR*, pages 8340–8348, 2018. 1, 2
- [3] Mingdeng Cao, Xintao Wang, Zhongang Qi, Ying Shan, Xiaohu Qie, and Yinqiang Zheng. Masactrl: Tuning-free mutual self-attention control for consistent image synthesis and editing. In *ICCV*, pages 22560–22570, 2023. 1, 2, 4
- [4] Caroline Chan, Shiry Ginosar, Tinghui Zhou, and Alexei A Efros. Everybody dance now. In *ICCV*, pages 5933–5942, 2019. 1, 2, 3
- [5] Aiyu Cui, Daniel McKee, and Svetlana Lazebnik. Dressing in order: Recurrent person image generation for pose transfer, virtual try-on and outfit editing. In *ICCV*, pages 14638–14647, 2021. 1, 2
- [6] Prafulla Dhariwal and Alexander Nichol. Diffusion models beat gans on image synthesis. *NeurIPS*, 34:8780–8794, 2021. 2, 3
- [7] Patrick Esser, Johnathan Chiu, Parmida Atighehchian, Jonathan Granskog, and Anastasis Germanidis. Structure and content-guided video synthesis with diffusion models. In *ICCV*, pages 7346–7356, 2023. 2
- [8] Songwei Ge, Seungjun Nah, Guilin Liu, Tyler Poon, Andrew Tao, Bryan Catanzaro, David Jacobs, Jia-Bin Huang, Ming-Yu Liu, and Yogesh Balaji. Preserve your own correlation:

- A noise prior for video diffusion models. In *ICCV*, pages 22930–22941, 2023. 2
- [9] Michal Geyer, Omer Bar-Tal, Shai Bagon, and Tali Dekel. Tokenflow: Consistent diffusion features for consistent video editing. *arXiv preprint arXiv:2307.10373*, 2023. 2, 4, 5, 6, 7
- [10] Ian Goodfellow, Jean Pouget-Abadie, Mehdi Mirza, Bing Xu, David Warde-Farley, Sherjil Ozair, Aaron Courville, and Yoshua Bengio. Generative adversarial nets. In *NeurIPS*, volume 27, 2014. 1
- [11] Shuyang Gu, Dong Chen, Jianmin Bao, Fang Wen, Bo Zhang, Dongdong Chen, Lu Yuan, and Baining Guo. Vector quantized diffusion model for text-to-image synthesis. In *CVPR*, pages 10696–10706, 2022. 2
- [12] Amir Hertz, Ron Mokady, Jay Tenenbaum, Kfir Aberman, Yael Pritch, and Daniel Cohen-Or. Prompt-to-prompt image editing with cross attention control. In *ICLR*, 2023. 2, 3
- [13] Jonathan Ho, William Chan, Chitwan Saharia, Jay Whang, Ruiqi Gao, Alexey Gritsenko, Diederik P Kingma, Ben Poole, Mohammad Norouzi, David J Fleet, et al. Imagen video: High definition video generation with diffusion models. *arXiv preprint arXiv:2210.02303*, 2022. 2
- [14] Jonathan Ho, Ajay Jain, and Pieter Abbeel. Denoising diffusion probabilistic models. In *NeurIPS*, volume 33, pages 6840–6851, 2020. 2, 3
- [15] Jonathan Ho, Tim Salimans, Alexey Gritsenko, William Chan, Mohammad Norouzi, and David J Fleet. Video diffusion models. *arXiv:2204.03458*, 2022. 2
- [16] Zhihao Hu and Dong Xu. Videocontrolnet: A motion-guided video-to-video translation framework by using diffusion model with controlnet. *arXiv preprint arXiv:2307.14073*, 2023. 4
- [17] Levon Khachatryan, Andranik Movsisyan, Vahram Tadevosyan, Roberto Henschel, Zhangyang Wang, Shant Navasardyan, and Humphrey Shi. Text2video-zero: Text-to-image diffusion models are zero-shot video generators. In *ICCV*, pages 15954–15964, 2023. 4, 5, 6
- [18] Diederik Kingma, Tim Salimans, Ben Poole, and Jonathan Ho. Variational diffusion models. In *NeurIPS*, volume 34, pages 21696–21707, 2021. 2
- [19] Diederik P Kingma and Max Welling. Auto-encoding variational bayes. In *ICLR*, 2014. 2
- [20] Yining Li, Chen Huang, and Chen Change Loy. Dense intrinsic appearance flow for human pose transfer. In *CVPR*, pages 3693–3702, 2019. 1, 2, 3, 4
- [21] Shaoteng Liu, Yuechen Zhang, Wenbo Li, Zhe Lin, and Jiaya Jia. Video-p2p: Video editing with cross-attention control. *arXiv preprint arXiv:2303.04761*, 2023. 2, 5, 6
- [22] Wen Liu, Zhixin Piao, Jie Min, Wenhan Luo, Lin Ma, and Shenghua Gao. Liquid warping gan: A unified framework for human motion imitation, appearance transfer and novel view synthesis. In *ICCV*, pages 5904–5913, 2019. 3
- [23] Liqian Ma, Xu Jia, Qianru Sun, Bernt Schiele, Tinne Tuytelaars, and Luc Van Gool. Pose guided person image generation. *NeurIPS*, 30, 2017. 1, 2
- [24] Yue Ma, Yingqing He, Xiaodong Cun, Xintao Wang, Ying Shan, Xiu Li, and Qifeng Chen. Follow your pose: Pose-guided text-to-video generation using pose-free videos. *arXiv preprint arXiv:2304.01186*, 2023. 1, 2, 5, 6
- [25] Ron Mokady, Amir Hertz, Kfir Aberman, Yael Pritch, and Daniel Cohen-Or. Null-text inversion for editing real images using guided diffusion models. In *CVPR*, pages 6038–6047, 2023. 3
- [26] Alexander Quinn Nichol, Prafulla Dhariwal, Aditya Ramesh, Pranav Shyam, Pamela Mishkin, Bob McGrew, Ilya Sutskever, and Mark Chen. Glide: Towards photorealistic image generation and editing with text-guided diffusion models. In *ICML*, pages 16784–16804, 2022. 1, 2
- [27] Chenyang Qi, Xiaodong Cun, Yong Zhang, Chenyang Lei, Xintao Wang, Ying Shan, and Qifeng Chen. Fatezero: Fusing attentions for zero-shot text-based video editing. In *ICCV*, pages 15932–15942, 2023. 2, 5, 6, 7
- [28] Aditya Ramesh, Mikhail Pavlov, Gabriel Goh, Scott Gray, Chelsea Voss, Alec Radford, Mark Chen, and Ilya Sutskever. Zero-shot text-to-image generation. In *ICML*, pages 8821–8831, 2021. 1, 2
- [29] Yurui Ren, Xiaoming Yu, Junming Chen, Thomas H Li, and Ge Li. Deep image spatial transformation for person image generation. In *CVPR*, pages 7690–7699, 2020. 1, 2
- [30] Robin Rombach, Andreas Blattmann, Dominik Lorenz, Patrick Esser, and Björn Ommer. High-resolution image synthesis with latent diffusion models. In *CVPR*, pages 10684–10695, 2022. 1, 2, 3, 4
- [31] Olaf Ronneberger, Philipp Fischer, and Thomas Brox. U-net: Convolutional networks for biomedical image segmentation. In *MICCAI*, pages 234–241, 2015. 3
- [32] Chitwan Saharia, William Chan, Saurabh Saxena, Lala Li, Jay Whang, Emily L Denton, Kamyar Ghasemipour, Raphael Gontijo Lopes, Burcu Karagol Ayan, Tim Salimans, et al. Photorealistic text-to-image diffusion models with deep language understanding. *NeurIPS*, 35:36479–36494, 2022. 1, 2
- [33] Aliaksandr Siarohin, Stéphane Lathuilière, Sergey Tulyakov, Elisa Ricci, and Nicu Sebe. First order motion model for image animation. In *NeurIPS*, pages 7137–7147, 2019. 2
- [34] Uriel Singer, Adam Polyak, Thomas Hayes, Xi Yin, Jie An, Songyang Zhang, Qiyuan Hu, Harry Yang, Oron Ashual, Oran Gafni, et al. Make-a-video: Text-to-video generation without text-video data. In *ICLR*, 2023. 2
- [35] Jiaming Song, Chenlin Meng, and Stefano Ermon. Denoising diffusion implicit models. In *ICLR*, 2020. 3
- [36] Ting-Chun Wang, Ming-Yu Liu, Jun-Yan Zhu, Guilin Liu, Andrew Tao, Jan Kautz, and Bryan Catanzaro. Video-to-video synthesis. In *NeurIPS*, volume 31, 2018. 1, 2
- [37] Jay Zhangjie Wu, Yixiao Ge, Xintao Wang, Stan Weixian Lei, Yuchao Gu, Yufei Shi, Wynne Hsu, Ying Shan, Xiaohu Qie, and Mike Zheng Shou. Tune-a-video: One-shot tuning of image diffusion models for text-to-video generation. In *ICCV*, pages 7623–7633, 2023. 1, 2, 3, 4, 5, 6
- [38] Haofei Xu, Jing Zhang, Jianfei Cai, Hamid Reza Tofighi, and Dacheng Tao. Gmflow: Learning optical flow via global matching. In *CVPR*, pages 8121–8130, 2022. 4
- [39] Shuai Yang, Yifan Zhou, Ziwei Liu, , and Chen Change Loy. Rerender a video: Zero-shot text-guided video-to-video translation. In *SIGGRAPH ASIA*, 2023. 1, 2, 4, 5, 6, 7
- [40] Lvmin Zhang, Anyi Rao, and Maneesh Agrawala. Adding conditional control to text-to-image diffusion models. In *ICCV*, pages 3836–3847, 2023. 1, 2, 3, 4, 6, 8
- [41] Yabo Zhang, Yuxiang Wei, Dongsheng Jiang, Xiaopeng

Zhang, Wangmeng Zuo, and Qi Tian. Controlvideo: Training-free controllable text-to-video generation. *arXiv preprint arXiv:2305.13077*, 2023. [2](#), [4](#), [5](#), [6](#), [7](#)

- [42] Min Zhao, Rongzhen Wang, Fan Bao, Chongxuan Li, and Jun Zhu. Controlvideo: Adding conditional control for one shot text-to-video editing. *arXiv preprint arXiv:2305.17098*, 2023. [1](#), [2](#), [4](#), [5](#), [6](#)